Supplement to **Age of air from in situ trace gas measurements: New techniques and insights**

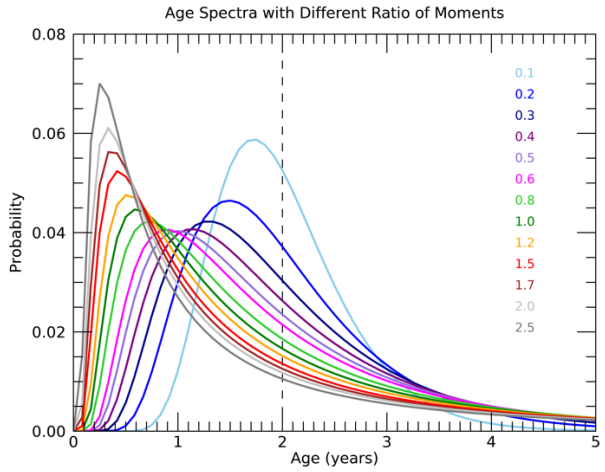

Figure S1. *Age spectra for a mean age of 2 years (dashed line) and ratio of moments ranging from 0.1-2.5.*

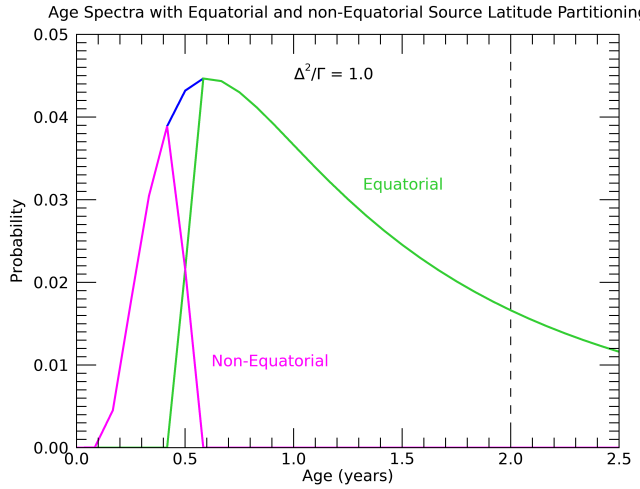

Figure S2. *Example age spectrum with the partitioning between the latitudinally varying surface source region (g_V) shown in magenta, the tropical surface source region (g_{TR}) shown in green and the total spectrum (G) shown in blue. This spectrum has a mean age of 2 years (indicated by the dashed line) and a ratio of moments of 1.*

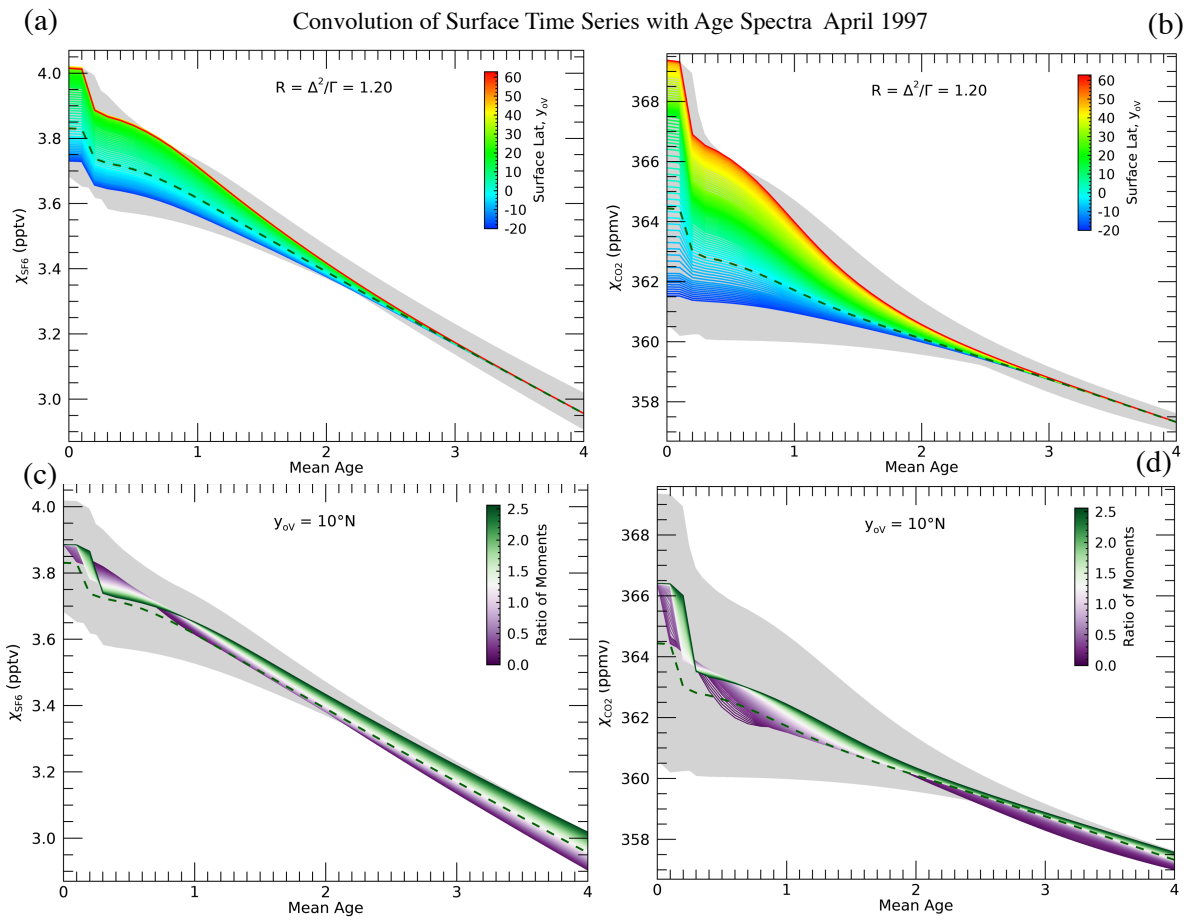

Figure S3. *Similar to Figure 2 in the main text but for April 1997.*

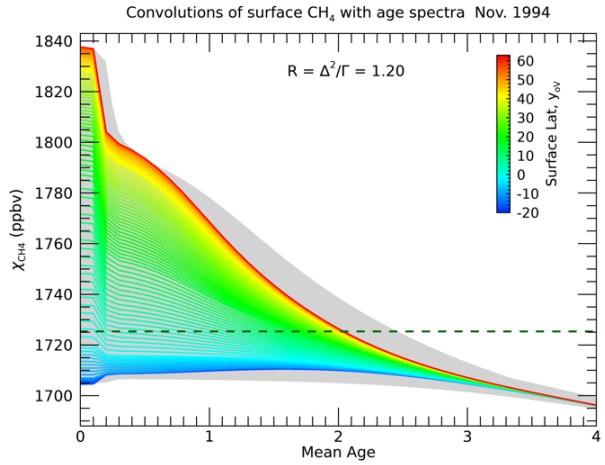

Figure S4. *Similar to Figure 2 in the main text but for CH_4 and only including the latitudinal dependence in colored lines. The surface average CH_4 mixing ratio at this time is indicated by the green dashed line.*

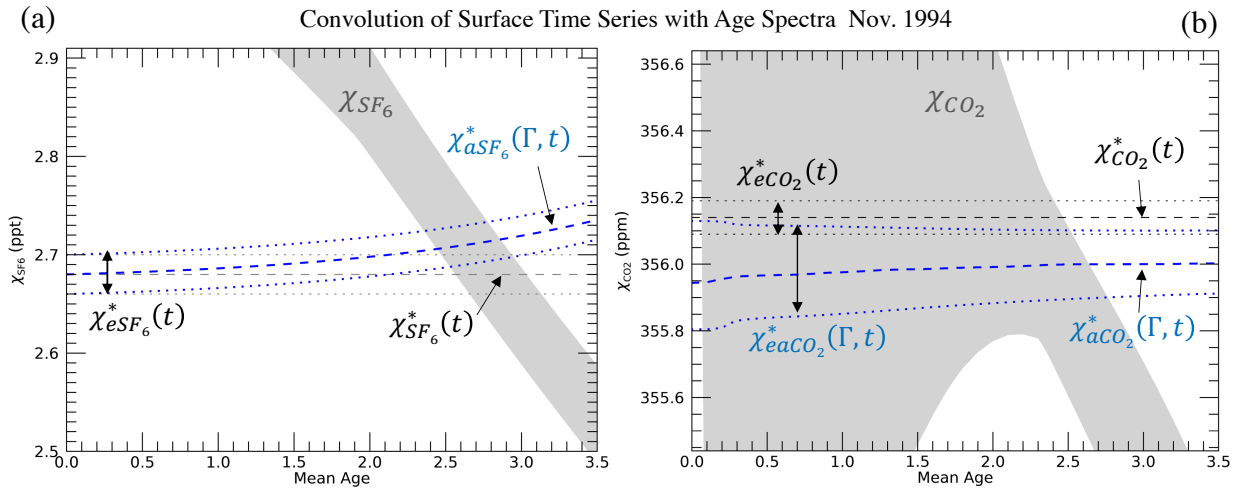

Figure S5. *Range of convolutions of SF_6 and CO_2 (grey shading) for the same time period as shown in Figure 1 but zoomed in on the mixing ratios around the values measured during the ER-2 flight of Nov. 4, 1994 at 1827 UTC during the ASHOE mission. The measured SF_6 mixing ratio is shown by the dashed black line in (a) and labeled $\chi^*_{SF6}(t)$ with uncertainty shown by the black dotted lines labeled $\chi^*_{eSF6}(t)$. The adjusted SF_6 mixing ratios are shown by the blue dashed line in (a) labeled $\chi^*_{aSF6}(\Gamma,t)$ are dependent on the mean age and increasingly deviate from the measured value with larger mean ages. The measured CO_2 mixing ratio is shown by the dashed black line in (b) and labeled $\chi^*_{CO2}(t)$ with uncertainty shown by the black dotted lines labeled $\chi^*_{eCO2}(t)$. The average adjusted CO_2 mixing ratios are shown by the blue dashed line in (b) labeled $\chi^*_{aCO2}(\Gamma,t)$ and are dependent on the mean age due to the dependence of the CH_4 boundary conditions on mean age as shown in Figure S4. There are actually a range of $\chi^*_{aCO2}(\Gamma,t)$ values for each mean age due to the range of convolved CH_4 mixing ratios for each mean age also shown in Figure S4. The uncertainty on the adjusted CO_2 shown by the blue dotted lines and labeled $\chi^*_{eaCO2}(\Gamma,t)$ is also a function of the mean age since it is based on the convolved CH_4 mixing ratios.*

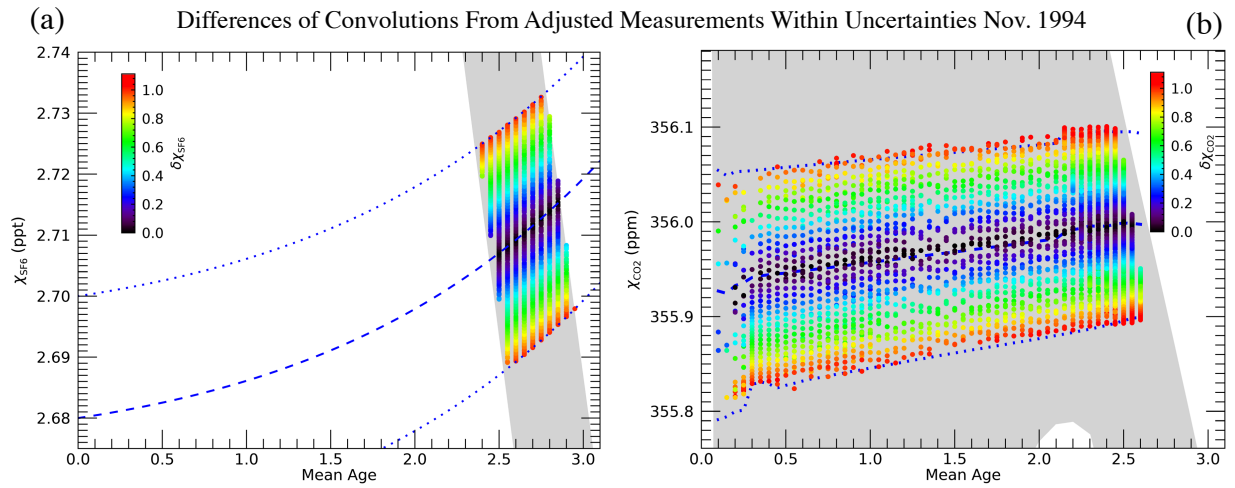

Figure S6. *Values of (a) $\delta\chi_{SF6}$ and (b) $\delta\chi_{CO2}$ where the surface convolutions χ_{SF_6} and χ_{CO_2} (grey shaded regions) agree within uncertainties with the values of χ^*_{aSF6} and χ^*_{aCO2} (blue dashed lines) respectively for the ER-2 flight of Nov 4, 1994 at 1827 UTC. The values of $\delta\chi_{SF6}$ and $\delta\chi_{CO2}$ are normalized by the values of χ^*_{eSF6} and χ^*_{eCO2} so they range from zero to one indicated by the color bar. The resolution of the convolutions is 0.05 years for mean age, 0.025 years for the ratio of moments and 10° for the latitudinal surface source region.*

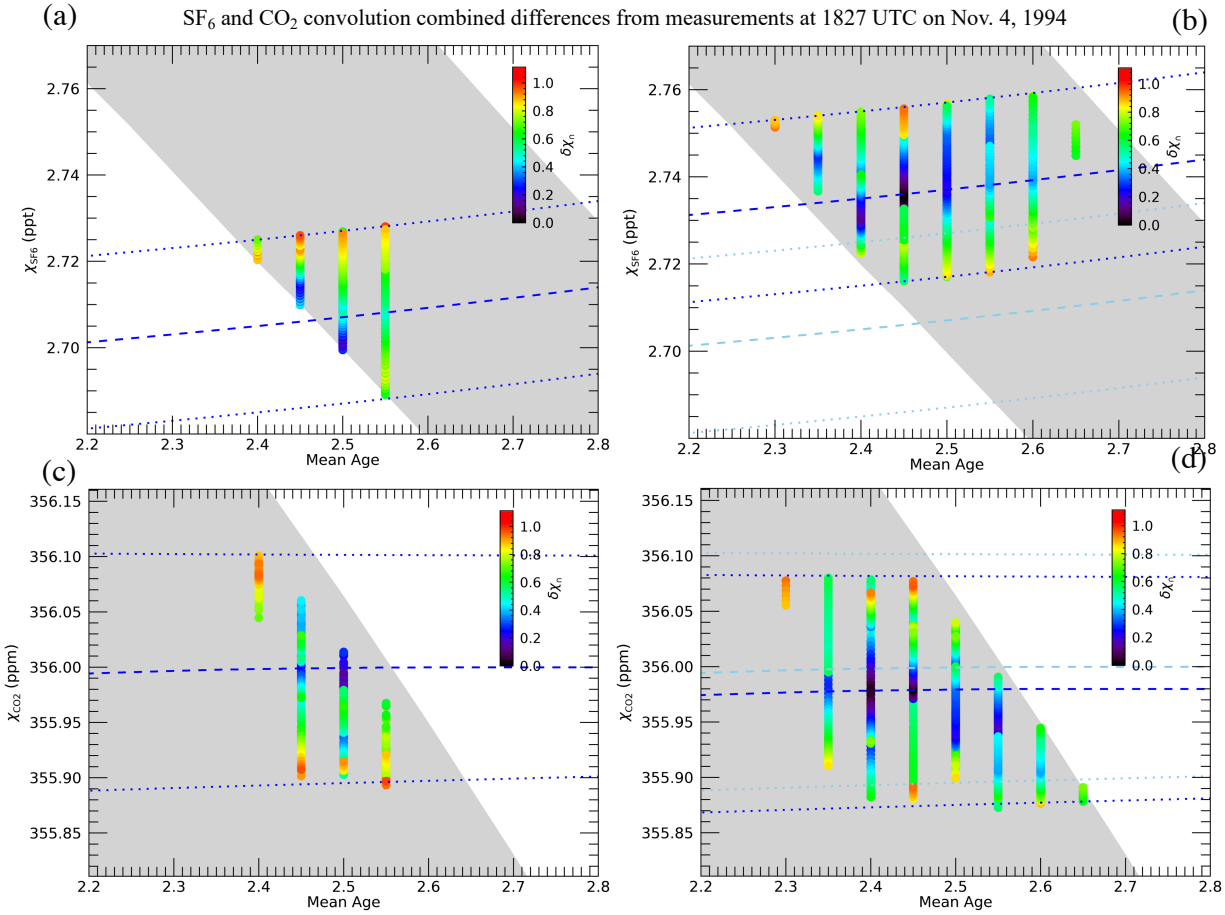

Figure S7. *Values of the combined differences for the intersection of solutions, $\delta\chi_{\cap}$, for the same ER-2 flight shown in previous figures. (a) and (c) show the results for the no offset ($\chi_{is} = 0$) and (b) and (d) the results for an optimized offset ($\chi_{SF6s} = 0.03\ ppt$ and $\chi_{CO2s} = -0.02\ ppm$). The blue dashed and dotted lines are the same as shown in Figure S5 for (a) and (c) and represent the offset values in (b) and (d). The light blue lines in (a) and (c) are the same as the blue lines in (a) and (c).*

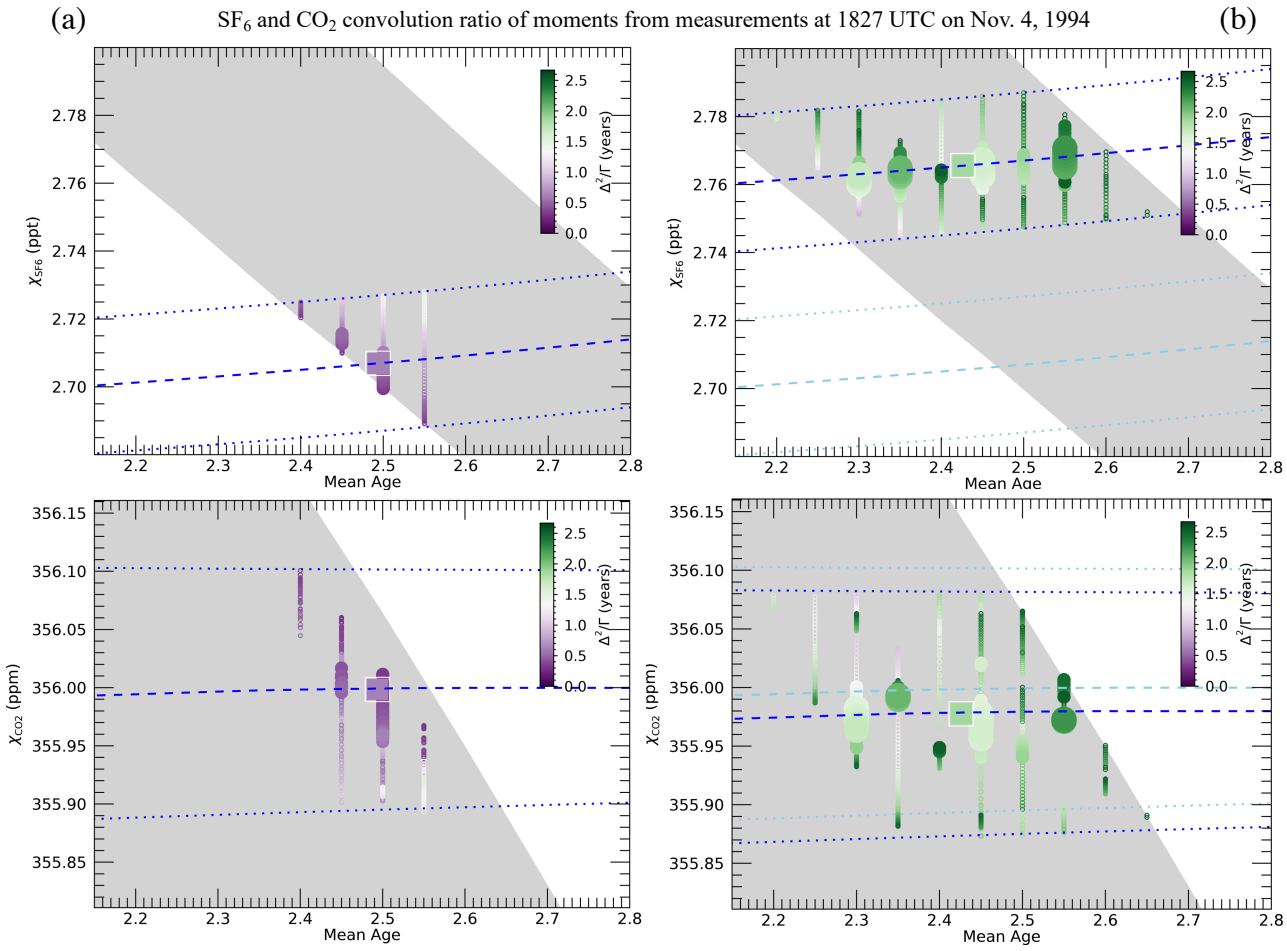

Figure S8. *Ratios of moments for the intersection of solutions, $\Delta_{\cap}^2/\Gamma_{\cap}$, for the same ER-2 flight time shown in previous figures. (a) and (c) show the results for no offset ($\chi_{is} = 0$) and (b) and (d) the results for an optimized offset ($\chi_{SF6s} = 0.03\ ppt$ and $\chi_{CO2s} = -0.02\ ppm$). The optimized solution for each case is shown by the square symbol. The blue lines are the same as described in Figure S7.*

Offset optimization technique

As mentioned in the main part of the manuscript, we perform an ensemble of optimizations over a range of offsets (χ_{is}) to the adjusted trace gas mixing ratios χ_{ai}^* for each measurement location. The full range of each ensemble spans from $-0.6\ ppt \leq \chi_{SF6s} \leq 0.6\ ppt$ with an interval of 0.03 ppt for SF_6 and $-0.15\ ppm \leq \chi_{CO2s} \leq 0.15\ ppm$ with an interval of 0.02 ppm for CO_2. There are conditions for which the entire ensemble is not considered for a particular set of measurements. Primarily we restrict the upper limit of χ_{SF6s} if enough $\delta\chi_{\cap min}(s) \leq 0.1$ are found for values of χ_{SF6s} near 0. This is the case for the November 1994 flight time shown in Figures S5-S9 where there is a wide range of mean ages from 0.1-2.6 years that agree with χ_{aCO2}^* within uncertainties (Fig. S6b). The values of $\Gamma_{\cap}$ with no offset to SF_6 ($\chi_{SF6s} = 0$) range from 2.4-2.55 years (Figure S7a,c). Offsetting SF_6 to larger mixing ratios results in younger values of $\Gamma_{\cap}$ (Fig. S9c) and agreement with CO_2 all the way to a mean age of 0.1 years for $\chi_{SF6s} = 0.6\ ppt$. This wide range of intersecting solutions with $\chi_{SF6s} > 0$ clearly defeats the purpose of

narrowing the possible solutions using two trace gases, which is why we place the upper limit on χ_{SF6s}.

To find the optimum offset values and associated transport parameters we further refine the ensemble set to only consider members with values of the minimum normalized combined difference $\delta\chi_{\cap min}(s) \leq 0.1$. This ensures a good agreement between χ_i and $\chi^*_{ai} + \chi_{is}$ for both trace gases and a wide range of transport parameters available to find an optimal solution set. For our example case, Figure S9a shows $\delta\chi_{\cap min}(s)$ for each member of the offset ensemble with many values less than 0.1 for $\chi_{SF6s} > 0$. We also consider the number of convolution values in each offset ensemble member with $\delta\chi_{\cap} \leq 0.1$ since this is a further indicator of agreement between the measured and convolved mixing ratios of both trace gases (Figure S9b). Only those members of the ensemble with at least five values of $\delta\chi_{\cap} \leq 0.1$ are included in the offset optimization. The results do not vary significantly with different values of this cutoff.

We perform an optimization with the identified set of offset ensemble members with a similar technique to that done for each member of the ensemble. In this case, we use the weighting function

$$W(s) = \frac{(\max(\delta\chi_{\cap min}) - \delta\chi_{\cap min}(s))^2}{\sum \delta\chi_{\cap min}(s)} \quad \text{(S1)}$$

so that those members of the ensemble with the smallest values of $\delta\chi_{\cap min}$ are weighted the most. After applying this weighting function on our example case, we find an optimum set of offset values to be $\chi_{SF6s} \approx 0.03$ ppt and $\chi_{CO2s} \approx -0.02$ ppm as shown by the small orange squares in Figure S9. The optimum values of the mean age and ratio of moments associated with these offsets are shown to be 2.41 and 1.57 years. Figure S9c shows that the mean ages vary only about a half year over all the offset values and are largely insensitive to the offset of CO_2. In contrast, the ratios of moments vary significantly from values of 0.4-2.2 over the offset range of SF_6 with again little dependence on the CO_2 offset.

The contrast in the intersection of solutions for this example case with no offset vs. the optimal offset is shown in Figures S7 and S8. The no offset case has a value of $\delta\chi_{\cap min}(s) = 0.15$, above our threshold of 0.1 to use in the offset optimization so it was not included. But since there is still a set of intersecting solutions, an optimal set of transport parameters can be calculated and the mean age and ratio of moments are 2.49 and 0.63 years. These would be the assumed solutions if no offset technique was performed. The mean age is very similar to the optimum offset value but the ratio of moments is much less.

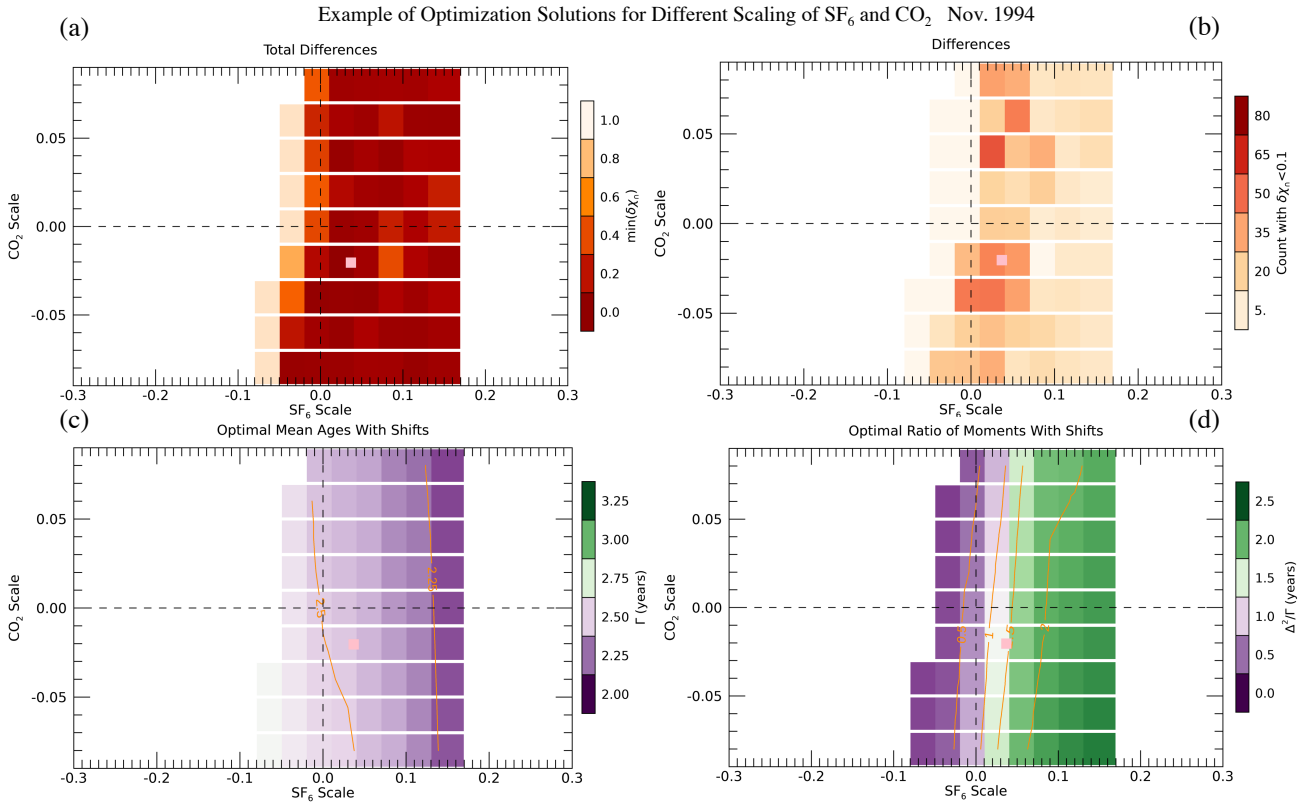

Figure S9. *Offset optimization results for the set of measurements during the same ER-2 flight of Nov. 4, 1994 as shown above. The x-axes represent the amount SF_6 was offset in ppt and the y-axis the amount CO_2 was offset in ppm. Each symbol represents the result of an individual optimization with the SF_6 and CO_2 offset. The parts of each plot with no symbols represent offset combinations where no intersection of solutions was found, such as for $\chi_{SF6s} < -0.1\ ppt$, or the offset was not performed, such as for $\chi_{SF6s} > 0.17\ ppt$. (a) shows the minimum combined difference values $\delta\chi_{\cap min}(s)$ (b) shows the number of convolution values with $\delta\chi_{\cap} \leq 0.1$, (c) the optimal mean ages and (d) the optimal ratios of moments. The optimal offset values are indicated by the orange symbol on each plot with $\chi_{SF6s} \approx 0.03\ ppt$ and $\chi_{CO2s} \approx -0.02\ ppm$.*

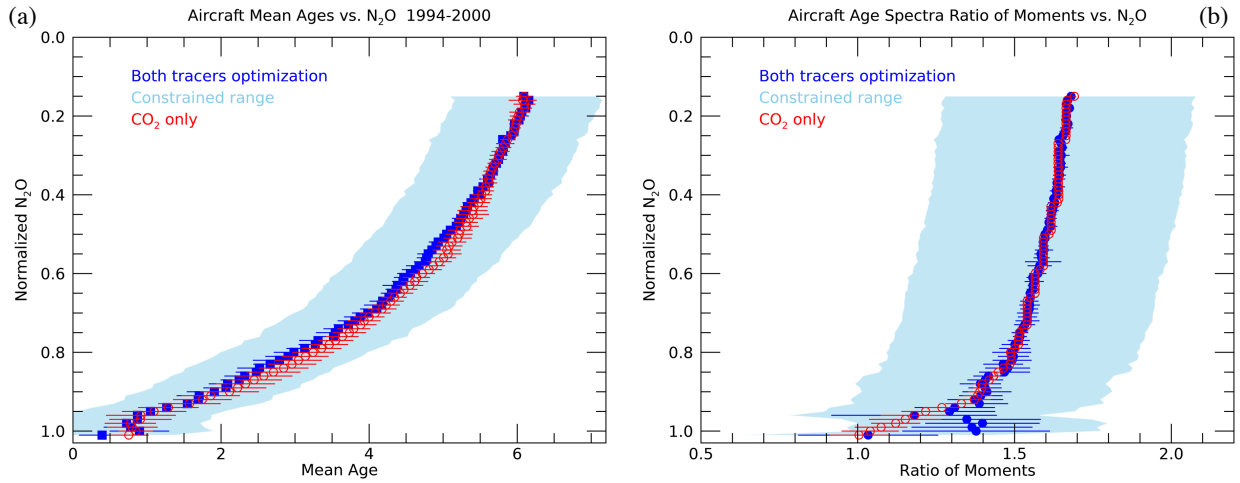

Figure S10. *Distribution of mean ages (a) and ratios of moments (b) for the 1990s aircraft measurements. The optimization results with both SF_6 and CO_2 are shown in the blue symbols and single trace gas optimizations with*

CO_2 in the red symbols. The constrained ranges used in the single trace gas optimization for this time period are shown in the light blue shading.

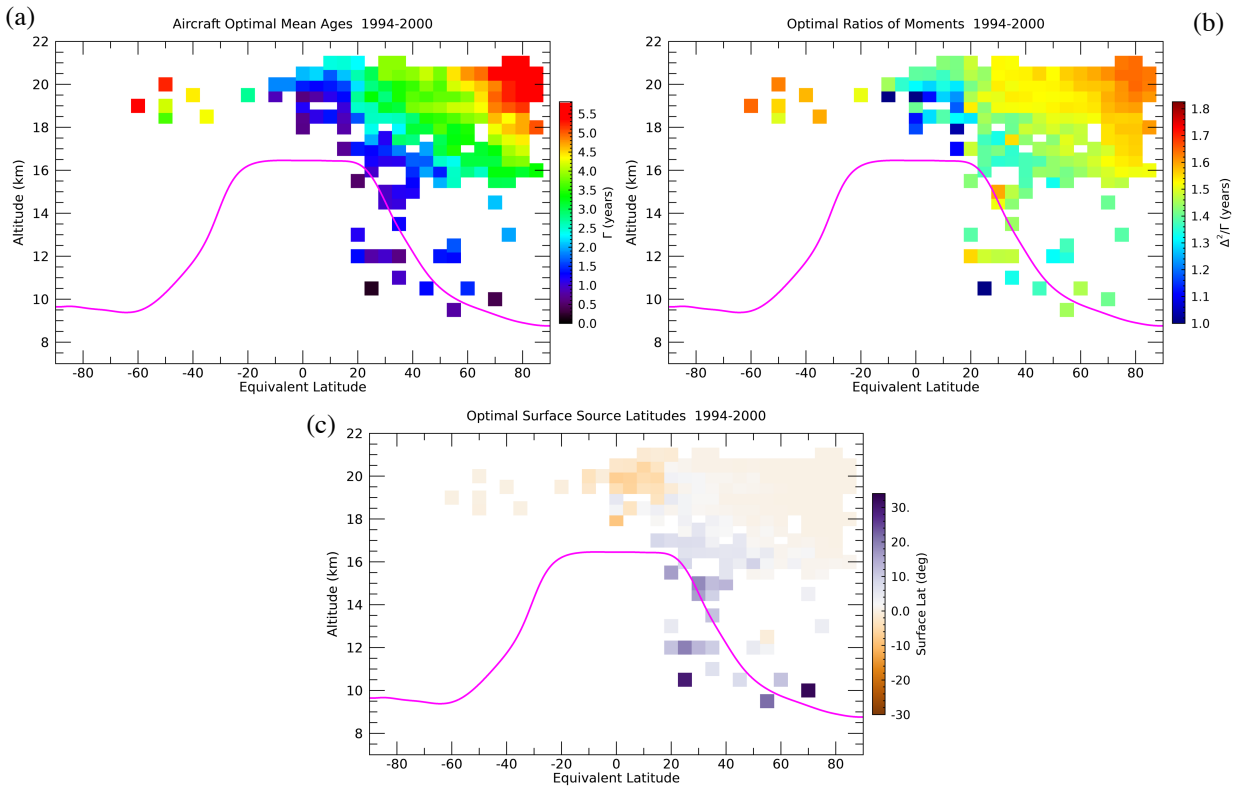

Figure S11. *Equivalent latitude vs. altitude distributions of mean ages (a), age spectra ratios of moments (b) and surface source latitudes (c) from the optimizations with SF_6 and CO_2 simultaneous measurements averaged over the 1990s aircraft missions.*

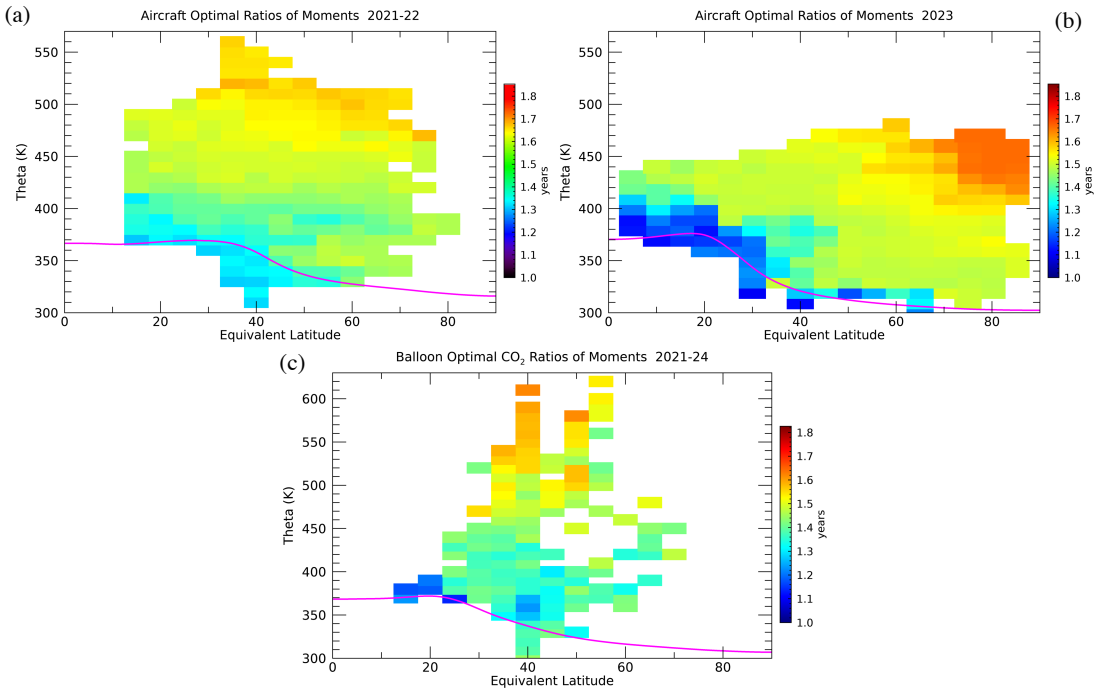

Figure S12. *Equivalent latitude vs. potential temperature distributions of ratios of moments from the DCOTSS (a), SABRE (b) and StratoCore (c) missions.*

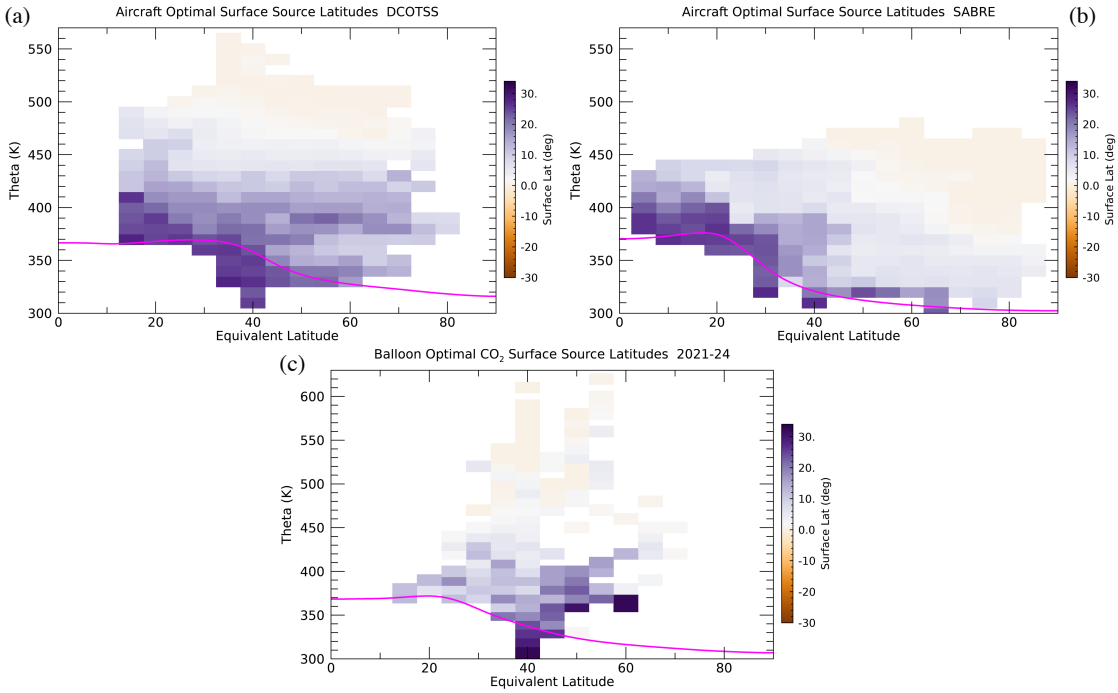

Figure S13. *Similar to Figure S12 but for surface source latitudes.*